An Unmixing-Based Change Detection Approach for Multiresolution Remote Sensing Images

Yasmine Kheira Benkouider and *Moussa Sofiane Karoui*

Centre des Techniques Spatiales, Arzew, Algeria

{ybenkouider, skaroui}@cts.asal.dz

ABSTRACT

In this paper, a new method is proposed to reveal changes using multiresolution and multitemporal remote sensing images. The considered method consists to provide two latent 2D variables with the same resolutions using the linear spectral unmixing concept based on nonnegative matrix factorization. Changes will then be discernible by comparing these two 2D variables or by applying classical change detection method, such as change vector analysis, on these variables. Simulation results presented show that the proposed approach is efficient for identifying changes occurred between two optical images with different spatial and spectral resolutions.

***Index Terms*—** Change detection, multiresolution and multitemporal remote sensing images, linear spectral unmixing, nonnegative matrix factorization

1. INTRODUCTION

Change detection is considered one of the most important issues in Earth observation [1], [2]. Detecting changes consists of locating regions that have evolved between two dates from two observations of the same scene [2]. Change monitoring through satellite imagery is useful in many applications such as land-use and land-cover change, urban change, forest change and damage assessment [3]. Ideally, the two images to be compared must have the same spatial and spectral resolutions or should be acquired from the same sensor, but in some emergency situations such as natural disasters, images from the same sensor are not available [2]. Therefore, exploiting the available data from different sources is inevitable. Many change detection algorithms have been developed for change detection using two observations with the same resolution such as post-classification comparison [4], change vector analysis [5], [6] and multivariate alteration detection technique [7].

Spatial and spectral resolutions difference between two image dates complicates direct comparison of data to detect changes. Recently, authors in [2], [8] and [9] propose fusion-based approaches to deal with images with different spatial and spectral resolutions.

The purpose of the research presented in this paper is to introduce and evaluate an algorithm to carry out change detection. The suggested strategy, consist at first to provide from two observed images with different spatial and spectral resolutions at two different moments, two latent 2D variables having the same spatial and spectral resolutions. The designed approach is based on the spectral unmixing concept using matrix factorization with nonnegativity constraints. The proposed algorithm uses a new gradient-based iterative update rules to optimize a cost function that includes observable data and spatial and spectral degradation models between them and unobserved ones. Then, changes detection is performed by comparing these restituted 2D variables or by applying a change vector analysis (CVA) [5], [6] approach to these generated variables.

The remainder of this paper is organized as follows: the proposed approach is presented in the second section. In the third section, simulation results are given and the performance is analyzed. Finally, conclusions are drawn in the last section of this paper.

2. PROPOSED APPROACH

In this section, the approach that we propose to detect changes is described. Consider two observed optical images acquired from two different sensors at two different dates. Typically, these two images are a hyperspectral image $X_h \in R_+^{L_h \times P_h}$ and a multispectral one $X_m \in R_+^{L_m \times P_m}$ with a number of pixels $P_m > P_h$ and a number of spectral bands $L_h > L_m$. Using a matrix form, the considered data can be modeled as [10], [11]

$$X_h = A_h S_h, \tag{1}$$

$$X_m = A_m S_m, \tag{2}$$

where each row of the matrix X_i is one spectral band of the considered hyperspectral/multispectral image. Every column of the matrices $A_h \in R_+^{L_h x K}$ and $A_m \in R_+^{L_m x K}$ is one hyperspectral/multispectral endmember-spectrum and the matrices $S_h \in R_+^{K x P_h}$ and $S_m \in R_+^{K x P_m}$ contains abundance fractions: each row represents all abundance fractions of one

endmember in all pixels. These abundance coefficients must satisfy the abundance sum-to-one constraint [10], [11]. K is the (known or estimated) number of endmembers.
Let X_m the before-change image acquired at T_1 and X_h the after-change image acquired at T_2. Due to the differences in spectral and spatial resolutions, the suggest method consists firstly to inferring two high spatial and spectral unobserved images $\tilde{Y}_1 \in R_+^{L_h \times P_m}$ and $\tilde{Y}_2 \in R_+^{L_h \times P_m}$, such as, X_m and X_h are respectively assumed to be spectrally and spatially degraded versions of the considered latent data:

$$X_m = D_\lambda \tilde{Y}_1, \tag{3}$$

$$X_h = \tilde{Y}_2 D_s, \tag{4}$$

where $D_\lambda \in R_+^{L_m \mathrm{x} L_h}$ and $D_s \in R_+^{P_m \mathrm{x} P_h}$ are linear operators that perform the spectral and the spatial degradation between observed and latent data. Consequently, $\tilde{Y}_1$, $\tilde{Y}_2, X_m$ and X_h can be modeled, in matrix form, as:

$$\tilde{Y}_1 = A_h S_m, \tag{5}$$

$$\tilde{Y}_2 = A_h S_{m'}, \tag{6}$$

$$X_m = D_\lambda A_h S_m, \tag{7}$$

$$X_h = A_h S_{m'} D_s, \tag{8}$$

where S_h is assumed to be the spatial degraded version of $S_{m'}$ (i.e. the two images X_m and X_h contain the same materials), and are linked according the following relation:

$$S_h = S_{m'} D_s. \tag{9}$$

In this work, an algorithm based on nonnegative matrix factorization (NMF) [10], [11] technique is used to estimate the latent images $\tilde{Y}_1$ and $\tilde{Y}_2$ from the observed images X_m and X_h by minimizing the designed cost function

$$J_1 = \frac{\alpha}{2}\left\|X_m - D_\lambda \tilde{A}_h \tilde{S}_m\right\|_F^2 + \frac{\beta}{2}\left\|X_h - \tilde{A}_h \tilde{S}_{m'} D_s\right\|_F^2, \tag{10}$$

where α and β are weighting coefficients that are set to the inverse of the number of elements in each considered norm [11]. $\|.\|_F$ represents the Frobenius norm.
The above J_I is minimized by an iterative gradient-based algorithm, which practically yields a monotonic decrease, from an iteration to another, of this cost function. To derive the gradient expressions, J_I is expressed as:

$$\begin{aligned} J_2 = & \frac{\alpha}{2} Tr(X_m X_m^T) - \alpha\, Tr\big(X_m \tilde{S}_m^T \tilde{A}_h^T D_\lambda^T\big) \\ & + \frac{\alpha}{2}\, Tr(D_\lambda \tilde{A}_h \tilde{S}_m \tilde{S}_m^T \tilde{A}_h^T D_\lambda^T) + \frac{\beta}{2}\, tr(X_h X_h^T) \\ & - \beta tr\big(X_h D_s^T \tilde{S}_{m'}^T \tilde{A}_h^T\big) + \frac{\beta}{2}\, tr(\tilde{A}_h \tilde{S}_{m'} D_s D_s^T \tilde{S}_{m'}^T \tilde{A}_h^T). \end{aligned} \tag{11}$$

Tr(.) and $(.)^{\mathrm{T}}$, respectively, represent the matrix trace and the matrix transpose. The gradient expressions of the considered criterion, with respect to the three involved variables, are therefore defined by:

$$\begin{aligned} \frac{\delta J_2}{\delta \tilde{A}_h} = & \alpha\big(D_\lambda^T D_\lambda \tilde{A}_h \tilde{S}_m \tilde{S}_m^T - D_\lambda^T X_m \tilde{S}_m^T\big) \\ & + \beta(\tilde{A}_h \tilde{S}_{m'} D_s D_s^T \tilde{S}_{m'}^T - X_h D_s^T \tilde{S}_{m'}^T), \end{aligned} \tag{12}$$

$$\frac{\delta J_2}{\delta \tilde{S}_m} = \alpha(\tilde{A}_h^T D_\lambda^T D_\lambda \tilde{A}_h \tilde{S}_m - \tilde{A}_h^T D_\lambda^T X_m), \tag{13}$$

$$\frac{\delta J_2}{\delta \tilde{S}_{m'}} = \beta(\tilde{A}_h^T \tilde{A}_h \tilde{S}_{m'} D_s D_s^T - \tilde{A}_h^T X_h D_s^T). \tag{14}$$

Since, the proposed algorithm is based on the gradient descent method with a fixed learning matrix rate φ_θ, the iterative update rule is defined by:

$$\theta \leftarrow \theta - \varphi_\theta \frac{\delta J_2}{\delta \theta}, \tag{15}$$

where θ corresponds to one of the three considered matrices. Applying this latter update rule is not sufficient since it does not guarantee the nonnegativity constraint. To ensure this constraint, a new iterative projected-gradient update rule can be derived from the above one. This new rule consists in replacing, if it is negative, each element of the left-hand side of (15) by a small positive number ε. The final iterative projected-gradient update rule is given by:

$$\theta \leftarrow \max\{\varepsilon, \theta - \varphi_\theta \frac{\delta J_2}{\delta \theta}\}. \tag{16}$$

Therefore, the final proposed iterative update rules for the considered matrices $\tilde{A}_h$, $\tilde{S}_m$ and $\tilde{S}_{m'}$ read

$$\tilde{A}_h \leftarrow \max\left\{\varepsilon, \tilde{A}_h - \varphi_{\tilde{A}_h} \frac{\delta J_2}{\delta \tilde{A}_h}\right\}, \tag{17}$$

$$\tilde{S}_m \leftarrow \max\left\{\varepsilon, \tilde{S}_m - \varphi_{\tilde{S}_m} \frac{\delta J_2}{\delta \tilde{S}_m}\right\}, \tag{18}$$

$$\tilde{S}_{m'} \leftarrow \max\left\{\varepsilon, \tilde{S}_{m'} - \varphi_{\tilde{S}_{m'}} \frac{\delta J_2}{\delta \tilde{S}_{m'}}\right\}. \tag{19}$$

As, the NMF based algorithm is sensitive to the initialization, the vertex component analysis (VCA) method [12] is performed to initialize estimated hyperspectral spectra $\tilde{A}_h^0$. Also, initial value of the matrix $\tilde{S}_m$ is obtained from multispectral data using the fully constrained least squares (FCLS) method [13]. The first approximation of $\tilde{S}_{m'}$ is obtained from the initial estimation of $\tilde{S}_m$ by applying a cubic interpolation.
The proposed algorithm is stopped when the number of iterations exceeds a predefined maximum number.

In these investigations, changes that have occurred are detected in two ways. In the first way, these changes are detected by using the obtained abundance fraction maps $\tilde{S}_m$ and $\tilde{S}_{m'}$. Indeed, a change map can be obtained by means of the following measure

$$\tilde{d} = \sqrt{\sum_{i=1}^{K} (\tilde{S}_{m'i} - \tilde{S}_{mi})^2}. \quad (20)$$

In the second way, changes are revealed by means of the standard CVA technique applied on the created latent unobserved images $\tilde{Y}_1$ and $\tilde{Y}_2$. The following measure is used to detect changes [14]

$$\tilde{d}_{cva} = \sqrt{\sum_{j=1}^{L_h} (\tilde{Y}_{2j} - \tilde{Y}_{1j})^2}. \quad (21)$$

3. EXPERIMENTAL RESULTS

In this section, the performance of the proposed approach is evaluated using realistic synthetic data.

3.1. Tested data

The multiresolution and multitemporal data used in this work are synthesized from Pavia University image captured by the Reflective Optics System Imaging Spectrometer (ROSIS) sensor, sized 492x183 pixels with 1.3 m spatial resolution and 103 spectral bands from 430 to 860 nm.
To generate observed data a simulation protocol inspired from [2] is conducted. At first, a pair of the observed before-after change datasets $X_{T_1} \in R_+^{L_h \times P_m}$ and $X_{T_2} \in R_+^{L_h \times P_m}$, are created by performing an unmixing-mixing process as follow:

$$X_{T_1} = A\, S_{T_1}, \quad (22)$$

$$X_{T_2} = A\, S_{T_2}, \quad (23)$$

where $A \in R_+^{L_h x K}$ is the matrix containing endmember spectra and $S_{T_i} \in R_+^{K x P_m}$ is the matrix of abundance fractions.
Then, in order to produce changes on X_{T_2}, original region abundances are replaced by abundance fractions of a region selected randomly producing a “copy-paste” pattern.

The image X_m is generated from X_{T_1} by applying a Gaussian blurring-decimation. Also, the image X_h is obtained from X_{T_2} by averaging the samples of the hyperspectral spectrum over the wavelength regions corresponding to the 4 bands Landsat-like spectral response.

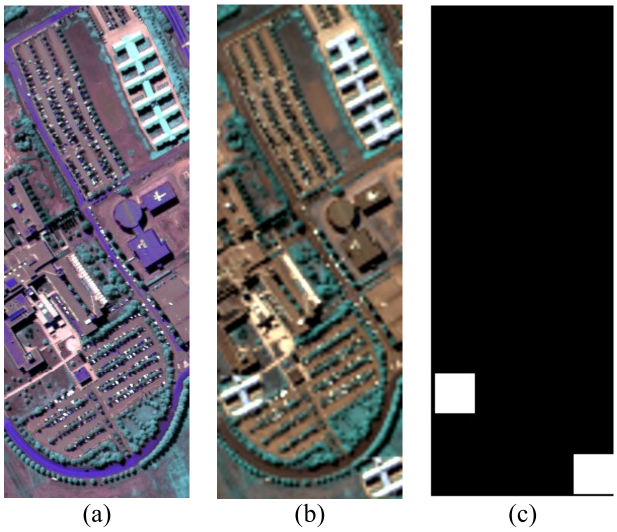

Fig.1. Created images: (a) X_m, (b) X_h, (c) the change mask.

3.2. Results and discussion

The proposed approach is applied to the generated data. Then, and as stated before, the changes can be detected by (20) or by performing a CVA approach to generated latent images by means of (21). These two ways are compared to another one, in which the unobserved latent images are obtained by adequately resampling the observed images.
To assess and compare changes detection results numerically, the percentage of correct detection (PCD) is used. This measure reflects the total proportion of pixels that are correctly predicted. Using the change map and the ground-truth change mask, the PCD is calculated as follow [15]

$$PCD = \frac{TP+TN}{TP+FP+TN+FN}, \quad (24)$$

where:
TP (true positives) is the number of change pixels correctly detected;
FP (false positives) is the number of no-change pixels incorrectly detected as change;
TN (true negatives) is the number of no-change pixels correctly detected;
FN (false negatives) is the number of change pixels incorrectly detected as no-change.

The obtained performances are reported in the following table by using different binarization thresholds.

Table I. Obtained results.

Threshold	**Proposed by means of (20)**	**Proposed by means of (21)**	**CVA on resampled observed images**
0	**3.55**	**3.55**	**3.55**
0.1	8.12	4.83	**12.60**
0.2	19.22	9.92	**23.84**
0.3	**39.62**	26.73	31.12
0.4	**61.83**	56.55	37.09
0.5	**81.71**	71.95	44.10
0.6	**89.40**	81.43	50.42
0.7	**92.39**	87.61	56.97
0.8	**94.08**	91.63	62.50
0.9	**95.57**	94.28	67.09
1	**96.03**	95.68	70.85

It can be observed from the above table, that the proposed approach, by means of the two ways, yields a satisfactory performance and, generally, outperforms the tested method that uses CVA on the resampled observed images. These results confirm that the proposed concept based on the linear spectral unmixing is a good strategy to change detection by using multiresolution and multitemporal remote sensing data.

4. CONCLUSION

In this article, a new method is proposed to deal with the remote sensing change detection problem. To reveal changes between two multitemporal and multiband images with different spatial and spectral resolutions, we have proposed to use the spectral unmixing concept based on nonnegative matrix factorization, in which, a new iterative update rules optimize a cost function that combines the two observed images and spatial and spectral degradation models between them and unobserved latent ones.

Two ways are proposed in these investigations. The first one uses change vector analysis on the obtained abundance fraction maps, while the second one uses this technique on the created unobserved latent images.

Obtained simulation results show that the proposed method is suitable for changes detection between multiresolution images.

5. REFERENCES

[1] M. Dalla Mura, S. Prasad, F. Pacifici, P. Gamba, J. Chanussot and J.A. Benediktsson, "Challenges and opportunities of multimodality and data fusion in remote sensing," *Proceedings of the IEEE*, vol. 103(9), pp. 1585-1601, 2015.

[2] V. Ferraris, N. Dobigeon, Q. Wei and M. Chabert, "Change detection between multi-band images using a robust fusion-based approach," *in Proc. of the IEEE International Conference on Acoustics, Speech and Signal Processing* (IEEE ICASSP 2017), New Orleans, USA, 2017.

[3] M. Hussain, D. Chen, A. Cheng, H. Wei and D. Stanley, "Change detection from remotely sensed images: From pixel-based to object-based approaches," *Journal of Photogrammetry and Remote Sensing*, vol. 80, pp. 91-106, 2013.

[4] L. Castellana, A. D'Addabbo and G. Pasquariello, "A composed supervised/unsupervised approach to improve change detection from remote sensing," *Pattern Recognition Letters,* vol. 28(4), pp. 405-413, 2007.

[5] F. Bovolo, S. Marchesi and L. Bruzzone, "A framework for automatic and unsupervised detection of multiple changes in multitemporal images," *IEEE Transactions on Geoscience and Remote Sensing*, vol. 50(6), pp. 2196-2212, 2012.

[6] F. Bovolo and L. Bruzzone, "An adaptive thresholding approach to multiple-change detection in multispectral images," *in Proc. of the IEEE International Geoscience and Remote Sensing Symposium* (IEEE IGARSS 2011), Vancouver, 2011.

[7] M. Frank and M. Canty, "Unsupervised Change Detection for Hyperspectral Images," *in 12th JPL Airborne Earth Science Workshop*, pp. 63-72, 2003.

[8] V. Ferraris, N. Dobigeon, Q. Wei and M. Chabert, "Detecting changes between optical images of different spatial and spectral resolutions: A fusion-based approach," *IEEE Transactions on Geoscience and Remote Sensing*, vol. 56(3), pp. 1566-1578, 2018.

[9] V. Ferraris, N. Dobigeon, Q. Wei, and M. Chabert, "Robust fusion of multiband images with different spatial and spectral resolutions for change detection," *IEEE Transactions on Computational Imaging*, vol. 3(2), pp. 175-186, 2017.

[10] M.S. Karoui, S. Hosseini, Y. Deville and A. Ouamri, "Modified Nonnegative Matrix Factorization for Endmember Spectra Extraction from Highly Mixed Hyperspectral Images Combined with Multispectral Data," *in Proc. of the IEEE International Conference on Acoustics, Speech and Signal Processing* (IEEE ICASSP 2017), New Orleans, USA, 2017.

[11] Y.K. Benkouider, M.S. Karoui, Y. Deville and S. Hosseini, “A New Multiplicative Nonnegative Matrix Factorization Method for Unmixing Hyperspectral Images Combined with Multispectral Data” *in Proc. of the 25th European Signal Processing Conference* (EUSIPCO 2017), Kos, Greece, 2017.

[12] J.M. Bioucas-Dias, A. Plaza, N. Dobigeon, M. Parente, Q. Du, P. Gader, and J. Chanussot, “Hyperspectral Unmixing Overview: Geometrical, Statistical, and Sparse Regression-Based Approaches,” *IEEE Journal of Selected Topics in Applied Earth Observations and Remote Sensing*, vol. 5(2), pp. 354-379, 2012.Approaches,” *IEEE Journal of Selected Topics in Applied Earth Observations and Remote Sensing*, vol. 5(2), pp. 354-379, 2012.

[13] D.C. Heinz, C.I. Chang, “Fully Constrained Least Squares Linear Spectral Mixture Analysis Method for Material Quantification in Hyperspectral Imagery,” *IEEE Transactions on Geoscience and Remote Sensing*, vol. 39(3), pp. 529-545, 2001.

[14] J. Chen, P. Gong, C. He, R. Pu, and P. Shi, “Land-use/land-cover change detection using improved change-vector analysis,” *Photogrammetric Engineering & Remote Sensing*, vol. 69, pp. 369-379, 2003.

[15] R. Radke, S. Andra, O. Al-Kofahi and B. Roysam, “Image change detection algorithms: A systematic survey,” *IEEE Transactions on Image Processing*, vol. 14, pp. 294-307, 2005.